Journal of Siberian Federal University. Engineering & Technologies 3 (2013 6) 257-267
~ ~ ~

УДК 669.713.17:537.84

Impact of Magnetohydrodynamic and Bubbles Driving Forces on the Alumina Concentration in the Bath of an Hall-Heroult Cell

Rene von Kaenel[a], Jacques Antille[a], Michel V. Romerio[b] and Olivier Besson[b]
[a] KAN-NAK Ltd.
35 B Route de Sion, 3960 Sierre, Switzerland
[b] University of Neuchâtel,
11 Emile Argand, 2000 Neuchatel, Switzerland

Received 15.05.2013, received in revised form 22.05.2013, accepted 31.05.2013

The alumina concentration in the bath plays a fundamental role on cell operation. Local depletion may lead to an anode effect when using carbon anodes. A mathematical model describing the alumina convection-diffusion process in the bath coupled to the cell magneto-hydrodynamic (MHD) in the presence of small bubbles is presented. Small bubbles may be assumed when slotted anodes are used. The relative importance of the velocity felds generated by the magnetic effects and/or the small bubbles on the alumina concentration in the bath is discussed.

Keywords: Alumina concentration modelling, gaz bubble interaction, MHD interaction

Introduction

The aluminum industry is continuously increasing the productivity of electrolysis cells by increasing the line current. In order to keep an acceptable anode current density, the anode length is almost systematically increased. As a result the central channel (distance between the anodes in the center of the cell) and the side channels (distance between the anodes to the side lining) are reduced. The channel geometry, Lorentz force fields and bubbles have an important impact on the bath velocity field. We will see that the velocity field plays a key role on the alumina distribution. In order to keep an acceptable energy input when increasing the current, the anode to cathode distance (ACD) is reduced as much as possible before reaching the Magneto-Hydrodynamic constraints. This means a further bath volume reduction. The increase of current imposes an increase of alumina feeding rate simultaneously with a reduction of bath volume. Therefore, the question of dissolution, diffusion and alumina transport becomes an important element for avoiding underfeeding leading to an increase of anode effects (AE) frequency. Alumina dissolution is a very complex phenomena in which the bath chemical composition, bath temperature, alumina temperature and alumina properties play an important role [1, 2, 3]. In this

* Corresponding author E-mail address: P.V.Polyakov@mail.ru

paper we assume that the dissolution is instantaneous when the alumina reaches the bath surface and concentrate the study on the diffusion and transport processes. The purpose of the study is to optimize the feeding quantities (feeding frequency), alumina feeders location and the number of feeders to minimize the number of AE and avoid sludge.

Bath velocity field in presence of bubbles and Lorentz force field: Theory

When the number of bubbles produced, per m^2 and per second, is too large, a numerical approach describing the motion of each bubble separately should be disregarded.

There are essentially two standard ways to overcome this difficulty. The first consists in performing some kind of averaging over the equations and over the corresponding fields. The second bypasses the averaging and directly postulates the flow equations for each phase.

One of the main difficulties encountered when performing an averaging process is related to the possible jumps that fields can suffer at the boundaries between the two phases. One way to overcome this problem, see for example [4], consists in extending the domain of definition of each motion equation to the domain occupied by the two phases. This is achieved by multiplying each equation by the characteristic function corresponding to its domain of definition. Derivatives are then performed in the sense of distributions allowing to keep track of these discontinuities in the averaging process.

Whatever choice we make, the resulting equations will contain terms which reflect the interaction between the two phases. The exact shape of these terms are not known; they have to be defined through constitutive equations.

Motion equations

Let Ω_l and Ω_g be the domains containing the fluid and the gas respectively, with corresponding characteristic functions χ_l and $\chi_g = 1 - \chi_l$. χ_l satisfies (see [4]),

$$\partial t\, \chi l + \mathrm{v} \cdot \nabla \chi l = 0, \tag{1}$$

where v is the velocity field. $< f >$ being the average of an arbitrary field f, we set

$$\alpha_{(l \text{ or } g)} = < \chi_{(l \text{ or } g)} >,\ \alpha_{(l \text{ or } g)} \widetilde{\mathrm{v}}_{(l \text{ or } g)} = < \chi_{(l \text{ or } g)} \mathrm{v} >, \tag{2}$$

and draw from (1) the averaging equation

$$\partial_t \alpha_{(l \text{ or } g)} + div\left(\alpha_{(l \text{ or } g)} \widetilde{\mathrm{v}}_{(l \text{ or } g)}\right) = 0. \tag{3}$$

Let ρ_l, ρ_g, T, j, g, B and $M^{i,j} = \frac{1}{\mu_0}\left(B^i B^j - \frac{1}{2} B^2 \delta^{ij}\right)$ be respectively the fluid and gas densities, the stress tensor, the electric current density, the gravitation force density, the magnetic induction and Maxwell tensor. Multiplying the MHD equations by the characteristic functions χ_l and χ_g and following the derivation used for (3) we get for the fluid and gas motions the equations

$$\left(\partial_t \alpha_t \widetilde{\mathrm{v}}_1 + < \nabla \cdot \left(\mathrm{v}_1 \otimes \mathrm{v}_1\right) > = \nabla\left(\alpha_l\left(\widetilde{T}_l + \widetilde{M}_l\right)\right) + \rho_l \alpha_l g - < \left(T_l + M_l\right) \cdot \nabla \chi_l >, \right. \tag{4}$$

$$\rho_g\left(\partial_t\alpha_g\widetilde{\mathrm{v}}_g+<\nabla\cdot\left(\mathrm{v}_g\otimes\mathrm{v}_g\right)>\right)=\nabla\cdot\left(\alpha_g\widetilde{T}_g\right)+\rho_l\alpha_g g-T_g\nabla\chi_g>, \tag{5}$$

where, for any f, $\alpha_{(l\text{ or }g)}\widetilde{f}_{(l\text{ or }g)}=<\chi_{(l\text{ or }g)}f>$.

Approximations and modeling

In order to have a tractable model we make the following assumptions.

$\rho_2 = 0$; the Reynolds tensor is included in the viscous term $\left(\alpha_l\widetilde{\tau}_l\right)$ with a change of the viscous constant which then becomes a diffusivity, (the notation will not be changed); we assume that (in T_l, T_g, $\widetilde{T}_l$ and $\widetilde{T}_g$) $p_l=\widetilde{p}_l=p_g=\widetilde{p}_g$.

In order to handle the averaging appearing in the equations we consider the different terms separately (without the indices). We also assume that Maxwell tensor is not affected by the averaging process. Setting

$$\mathrm{v}=\widetilde{\mathrm{v}}+\mathrm{w},\quad\text{so that}\quad<\chi_J\,\mathrm{w}>=0, \tag{6}$$

one gets

$$\chi_l\mathrm{v}\otimes\mathrm{v}=\alpha_l\widetilde{\mathrm{v}}\otimes\widetilde{\mathrm{v}}-\alpha_l T^{Re}, \tag{7}$$

where $\alpha_l T^{Re}=-<\chi_l\mathrm{w}\otimes\mathrm{w}>$. Setting $T=(-pI+\eta\tau(\mathrm{v}))$, where $\tau(\mathrm{v})=\nabla\mathrm{v}+(\nabla\mathrm{v})^t$ we finally note that

$$<\chi_l T>=<\chi_l\left(-pI+\eta\tau(\mathrm{v})\right)>=\alpha_l\widetilde{p}I+\eta\alpha_l\tau(\widetilde{\mathrm{v}}). \tag{8}$$

Taking these approximations into account the equations (4) and (5) become

$$\begin{aligned}\rho_l\left(\partial_t\left(\alpha_l\widetilde{\mathrm{v}}_1\right)+\nabla\cdot\left(\alpha_l\widetilde{\mathrm{v}}_1\otimes\widetilde{\mathrm{v}}_1\right)\right)=&-\alpha_l\nabla\widetilde{p}_1+\nabla\cdot\left(\alpha_l\widetilde{\tau}_1\right)+\alpha_l\nabla\cdot\widetilde{\mathrm{M}}_1+\rho_l\alpha_l g-\\&-<\tau_1\cdot\nabla\chi_l>,\end{aligned} \tag{9}$$

$$-\alpha_g\nabla\widetilde{p}_g+\nabla\cdot\alpha_g\widetilde{\tau}_g=<\tau_g\nabla\chi_g>. \tag{10}$$

Neglecting the surface tension effect and handling the jump conditions between the two phases in the setting used for the equations we get

$$\widetilde{\mathrm{v}}_g-\widetilde{\mathrm{v}}_l=\widetilde{\mathrm{v}}_{slip}\ \text{and}\ <\left(\tau_1-\tau_g\right)\cdot\nabla\chi_l>=0, \tag{11}$$

where $\widetilde{\mathrm{v}}_{slip}$ is a new field which takes into account for the averaging on the jump conditions.

Second approximation

We now make the following assumptions

$$\nabla\cdot\left(\alpha_g\widetilde{\tau}_2\right)=0. \tag{12}$$

and

$$div\left(\alpha_l\mathrm{v}_{slip}\right)=0. \tag{13}$$

We moreover introduce the new field f_{int} defined by

$$f_{int}=<\tau_2\cdot\nabla\chi_g>=<\tau_1\cdot\nabla\chi_g>. \tag{14}$$

With this assumption (10) becomes

$$-\alpha_g \nabla \tilde{p}_2 + f_{int} = 0. \tag{15}$$

From (3) and (13) one draws

$$div\, \mathrm{v}_1 = 0. \tag{16}$$

$$\partial_t \alpha_g + div\left(\alpha_g \tilde{\mathrm{v}}_g\right) = 0. \tag{17}$$

Constitutive equations

We will now make the assumption that the field (14), i.e. f_{int}, is a function of $\tilde{\mathrm{v}}_{slip}$ only.

Following [5] we assume that

$$f_{int} = \lambda \alpha_g \tilde{\mathrm{v}}_{slip}, \tag{18}$$

where λ is a constant. Introducing this expression into (15) yields, since by assumption $\tilde{p}_1 = \tilde{p}_2$,

$$-\alpha_g \nabla \tilde{p}_1 = \lambda \alpha_g \tilde{\mathrm{v}}_{slip}. \tag{19}$$

so that

$$\tilde{\mathrm{v}}_{slip} = -\frac{\nabla \tilde{p}_1}{\lambda}. \tag{20}$$

The coefficient λ has to be determined experimentally.

The model

With the above results we are now ready to give the equations on which our model is leaning. Fluid averaged equations

$$div\, \mathrm{v}_1 = 0. \tag{21}$$

$$\rho_l\left(\partial_t\left(\alpha_l \tilde{\mathrm{v}}_1\right) + \nabla \cdot \left(\alpha_l \tilde{\mathrm{v}}_1 \otimes \tilde{\mathrm{v}}_1\right)\right) = -\nabla \tilde{p}_1 + \nabla \cdot \left(\alpha_l \tilde{\tau}_1\right) + \alpha_l \nabla \cdot \tilde{\mathrm{M}}_1 + \rho_l \alpha_l g. \tag{22}$$

Gas averaged equations

$$\partial_t \alpha_g + div\left(\alpha_g \tilde{\mathrm{v}}_2\right) = 0, \tag{23}$$

$$\alpha_g \nabla \tilde{p}_1 + \alpha_g \lambda \tilde{\mathrm{v}}_{slip} = 0. \tag{24}$$

Jump averaged conditions

$$\tilde{\mathrm{v}}_2 = \tilde{\mathrm{v}}_1 + \tilde{\mathrm{v}}_{slip}, \tag{25}$$

$$\alpha_l + \alpha_g = 1. \tag{26}$$

Boundary conditions on the different fields have to be added.

Alumina diffusion and convection: Theory

Let $\Omega \subset R^3$ be the domain representing the cell, Ω_b be the bath, and Ω_a the anodes.

Current density

The current density distribution in the bath is a function of alumina concentration, and is given by

$$j = -\sigma(c)\nabla\phi \tag{27}$$

ϕ where is the potential, and σ is the electrical conductivity, which depends on the alumina concentration *c*.

Since diυ j = 0, we get

$$-div(\sigma(c)\nabla\phi) = 0 \tag{28}$$

with following the boundary conditions ($j \square n$) = j_0 on the anodic rod, $\phi = 0$ on the bath-metal interface,

and $\sigma(c)\frac{\partial\phi}{\partial n} = 0$ elsewhere.

The current $j = (j_1; j_2; j_3)$ is then computed in the following way to avoid rough approximations.

$$\int_\Omega j_l \psi dx = -\int_\Omega \sigma(c)\frac{\partial\phi}{\partial x_l}\psi dx \tag{29}$$

for suitable functions ψ, and l = 1; 2; 3.

The model will take into account the analysis of the parameter σ as a function of the bath composition.

Alumina distribution

In this study, it is assumed that the alumina feeding is known, and that the dissolution is instantaneous. The alumina distribution in the bath Ω_b is given by the following partial differential equation

$$\frac{\partial c(x,t)}{\partial t} - div(\alpha(x,t))\nabla c(x,t) + (v(x,t)|\nabla c(x,t)) = 0, \tag{30}$$

where

– *c* is the alumina concentration in mol/m^3,

– α is the anisotropic diffusion coefficient. A value of 0,5 m^2/s was determining the Reynolds mean tensor. It also leads to an average alumina concentration reflecting industrial cells.

– v is the velocity field in Ω_b induced by the bubble motion, and the MHD.

The boundary and initial conditions have the following form.

– The concentration *c* is given on the feeder.

– The concentration flux on the anode and the bath-aluminum interface is $\alpha\frac{\partial c}{\partial n} + \beta(j|n) = 0$; the coe

cient β verify $\beta = \frac{1}{zF}$ if $[c] = mol/m^3$, with *z* is the valence, and *F* is the Faraday constant, in our case *z* = 6.

– $\alpha\frac{\partial c}{\partial n} = 0$ elsewhere,

– c is given at time $t = 0$.

Weak formulation

Let us use the following notations.

– Γ_b is the bottom of the cell (the metal-bath interface),

– Γ_a is the top of the anodic rod (the entrance of the current),

– Γ_f is the feeder domain,

– Γ_{ab} is the interface between the anode and the bath.

With these notations, set

$$V = \{\psi \in H^1(\Omega),\ \psi = 0 \text{ on } \Gamma_b\}, \tag{31}$$

equipped with the norm $|\psi| = |\psi|_V = \|\nabla\psi\|_{L^2(\Omega)}$

$$W = \{\psi \in H^1(\Omega_b),\ \psi = 0 \text{ on } \Gamma_f\}, \tag{32}$$

equipped with the norm $|\psi| = |\psi|_W = \|\nabla\psi\|_{L^2(\Omega_b)}$.

The weak formulation of problem (28) is:

Find $\phi \in V$ such that, $\forall\psi \in V$,

$$\int_\Omega (\sigma(c)\nabla\phi|\nabla\psi)\,dx = \int_{\Gamma_a} j_0\psi\,d\sigma. \tag{33}$$

Then the computation of the current density $j = (j_1; j_2; j_3)$ is obtained from equation (29) $\forall\psi \in L^2(\Omega)$. Finally, the weak formulation for the alumina concentration is: Find $c \in L^2\left(0,T;H^1(\Omega_b)\right)$ with $c = c_f$ on F_f, such that $\forall\psi \in W$,

$$\int_{\Omega_b}\left(\frac{\partial c}{\partial t} + (\mathbf{v}|\nabla c)\right)\psi\,dx + \int_{\Omega_b}(\alpha\nabla c|\nabla\psi)\,dx = -\beta\int_{\Gamma_{ab}\cup\Gamma_b}|(j|n)|\psi\,d\sigma. \tag{34}$$

Numerical methods

Let us decompose the domains Ω, and Ω_b into classical tetrahedral finite element mesh. For the numerical simulations of problems (33), (29), and (34), the following algorithm is used.

– **Initialization**

An initial alumina concentration distribution c_0 is given at time $t = 0$. Let τ be the time step.

– **Iterations**

For time $t_m = m \cdot \tau$, if c_h^m is the concentration at time t_m

a) Compute the electrical conductivity $\sigma = \sigma\left(c_h^m\right)$

b) Find $\phi_h \in V_h$ such that, $\forall\psi \in V_h$,

$$\int_\Omega (\sigma\nabla\phi_h|\nabla\psi)\,dx = \int_{\Gamma_a} j_0\psi\,d\sigma. \tag{35}$$

c) The electric current $j_h = (j_h;1; j_h;2; j_h;3)$ is obtained as, $\forall l = 1; 2; 3$, and $\forall\psi \in Z_h$,

$$\int_\Omega j_{h,l}\psi = -\int_\Omega \sigma(c)\frac{\partial\phi_h}{\partial x_l}\psi\,dx. \tag{36}$$

d) A BDF scheme of order 2 [6] is used for the time discretization of the concentration equation (34). Moreover a Petrov-Galerkin streamline diffusion method is applied for the advection term [7, 8]. We get the following equation (δ small parameter).

Find c_h^{m+1}, solution of

$$\int_{\Omega_b} 1.5\frac{c_h^{m+1}}{\tau}(\psi+\delta(\nabla\psi|\mathbf{v}))\,dx+\int_{\Omega_b}(\alpha\nabla c_h^{m+1}|\nabla\psi)\,dx+$$
$$\int_{\Omega_b}(\mathbf{v}|\nabla c_h^{m+1})(\psi+\delta(\nabla\psi|\mathbf{v}))\,dx=-\beta\int_{\Gamma_{ab}\cup\Gamma_b}|(j|n)|\psi\,d\sigma+ \qquad (37)$$
$$\int_{\Omega_b}\frac{2c_h^m-0.5c_h^{m-1}}{\tau}(\psi+\delta(\nabla\psi|\mathbf{v}))\,dx.$$

for all $\psi\in W_h$

Alumina diffusion and convection: Industrial cell

In this section some numerical result for the computation of the alumina distribution in the bath are presented. On the feeders, the alumina concentration is set to 5 % of the bath weight. As a stationary solution is presented, continuous feeding is assumed. The impact of dump feeding could easily be analysed.

Figure 1 correspond to the stationary alumina distribution, when the velocity is neglected. The concentration is shown under the anodes. The two feeders locations appear clearly in the figure. The asymmetry of the diffusion pattern reflects the larger channel width at the feeders. Figure 2 shows the alumina concentration under the same conditions at metalbath interface level. Away from the feeders, at a distance larger than about one anode width, the concentration is close to 2,55 %. The vertical variation of the alumina concentration is 0:5 % under the feeders. It is negligible away from the feeders.

In fig. 3, the velocity streamlines induced by the MHD are presented.

The impact of this velocity field is shown in fig. 4.

The previous cases did not take the bubbles into account. It is well known that they have an important effect on the velocity field. Moreover the considered cell has slotted anodes. This also has an

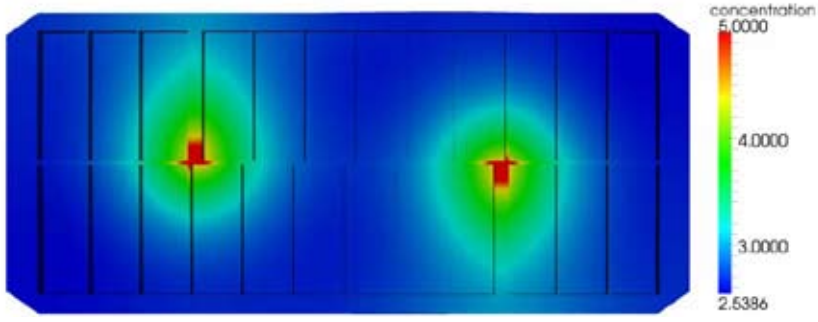

Fig. 1. Alumina concentration in the bath when the velocity is zero, under the anodes

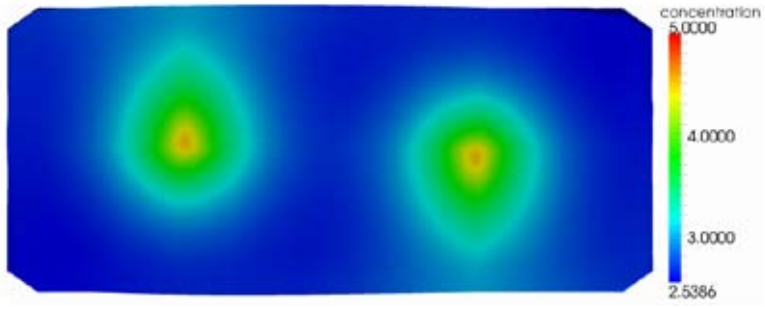

Fig. 2. Alumina concentration in the bath when the velocity is zero, bath-metal interface

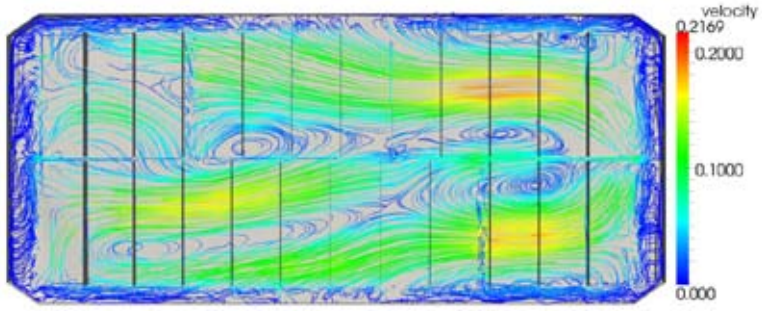

Fig. 3. MHD velocity in the bath (streamlines)

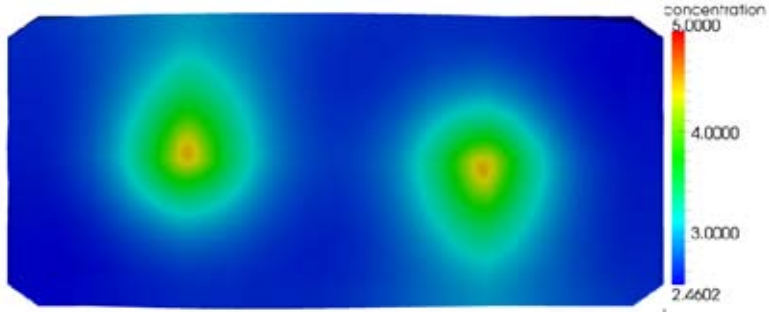

Fig. 4. Alumina concentration in the bath when the velocity is induced by the MHD

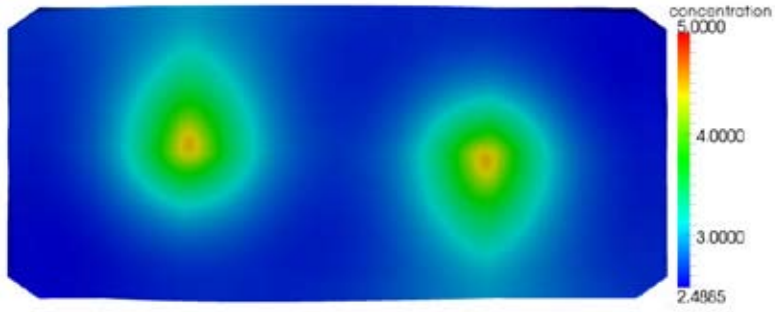

Fig. 5. Alumina concentration in the bath, velocity induced by MHD, bubbles, and slots

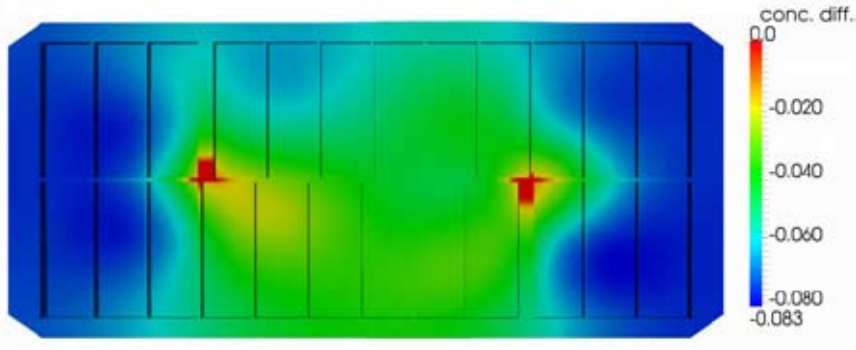

Fig. 6. Alumina concentration variation due to MHD [%]

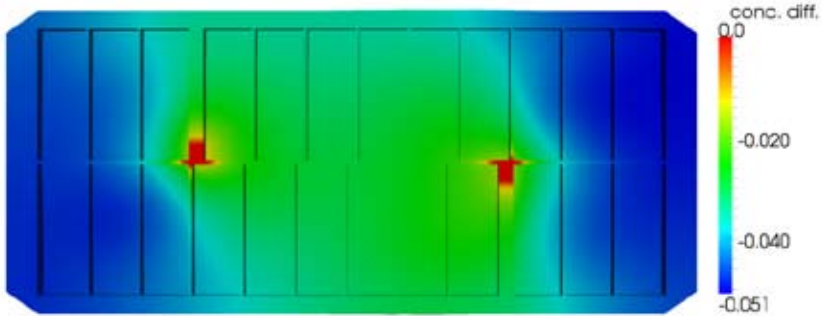

Fig. 7. Alumina concentration variation due to MHD, bubbles, and slots [%]

impact on the velocity. Figure 5 considers the case when the velocity field consists of the effects of the MDH, the bubbles, and the slots in the anodes.

From the different figures, the alumina concentration field appears as slightly modified by the velocity field. However, when considering the concentration evolution, the time needed for reaching the stationary state is reduced by a factor 2 in any situation when the velocity field is acting. Therefore the velocity field plays an important role in the feeding process (alumina dumps).

To highlight the role of the velocity field, fig. 6 and 7 show the difference between the alumina concentration field due to the diffusion only and in presence of MHD velocity, resp. total velocity field.

The highest diaaerences are observed at the ends of the cell, due essentially to the MHD effects. High negative values relate to high alumina concentration difference. The effect of bubbles and slots generate turbulence, homogenizing the concentration distribution.

Conclusions

A new model for the velocity field in presence of MHD, and small bubbles is developed. This velocity field is used to determine the evolution of the alumina concentration using a non-stationary convection-diffusion equation. This equation takes into account the feeding, and the Faraday law at the anodes and cathode.

The application to an existing cell with two point feeders demonstrate the following:

– The alumina concentration can vary up to 2,5 %. Typically a variation 1 % can be expected between anodes.

– The time needed to reach the stationary state due to the diffusion process only is twice the one for the case with MHD and bubbles effects velocity fields. It was found around two minutes.

– The velocity field has an important effect for the alumina distribution under the anodes. It helps to homogenize the alumina concentration.

– Bubbles and slots modify the velocity field which generate turbulences leading to increased homogenizing effects.

References

[1] *Kobbeltvedt O., Rolseth S., Thonstad J.* // Department of Electrochemistry, Norwegian Institute of Technology, N-7034 Trondheim, Norway SINTEF Materials Technology, N7034 Trondheim, Norway.

[2] *Haverkamp R.G.* // PhD Thesis, University of Auckland (1992).

[3] *Kobbeltvedt O., Rolseth S., Thonstad J.* // Light Metals, TMS, 1996.

[4] *Drew D.A. and Passman S.L.* Theory of Multicomponent Fluids. Spinger 1999.

[5] *Panescu F.R.G.* // Inria Sophia: Antipolis, 2006.

[6] *Hairer E., Nrstett S.P., Wanner G.* Solving Ordinary Differential Equations I. Springer-Verlag, 1987.

[7] *Johnson C., Saranen J.* // Math. of Comp. 47. (1986). P. 118.

[8] Franca L.P., Hauke G., Masud A. // Comput. Methods Appl. Mech. Engrg. 195. (2006). P. 1560–1572.

Влияние магнитогидродинамической силы и силы, обусловленной движением пузырьков, на концентрацию глинозёма в ванне Эру-Холла

Rene von Kaenel[a], Jacques Antille[a], Michel V. Romerio[б], Olivier Besson[б]
[a]KAN-NAK Ltd.
Route de Sion 35 B, 3960 Sierre, Switzerland
[б]University of Neuchâtel,
Emile Argand 11, 2000 Neuchatel, Switzerland

Концентрация глинозёма в алюминиевом электролизере играет ключевую роль в технологических операциях. Локальное истощение может привести к анодному эффекту при использовании углеродных анодов. Представлена математическая модель, описывающая конвективно-диффузионный перенос глинозёма, связанный с магнитогидродинамикой (МГД) в ванне при малых размерах пузырьков. Маленькие пузырьки можно получить при использовании анодов с пазами. Обсуждена относительная значимость полей скоростей, создаваемых магнитными эффектами и/или маленькими пузырями, на концентрацию глинозёма в электролизере.

Ключевые слова: моделирование концентрации глинозёма, взаимодействие газовых пузырьков, магнитогидродинамическое взаимодействие.